



## OPEN

SUBJECT AREAS:  
ORGANOGENESIS  
DISEASE MODELReceived  
7 March 2014Accepted  
20 June 2014Published  
7 July 2014Correspondence and  
requests for materials  
should be addressed to  
L.L. (alilir@swu.edu.  
cn; swu\_lili@126.com)\* These authors  
contributed equally to  
this work.

# Acetylcholine serves as a derepressor in Loperamide-induced Opioid-Induced Bowel Dysfunction (OIBD) in zebrafish

Yanyan Shi\*, Yu Zhang\*, Fangying Zhao, Hua Ruan, Honghui Huang, Lingfei Luo &amp; Li Li

The State Key Laboratory Breeding Base of Bioresources and Eco-environments, Key Laboratory of Freshwater Fish Reproduction and Development, Ministry of Education, Laboratory of Molecular Developmental Biology, School of Life Sciences, Southwest University, Beibei, 400715 Chongqing, China.

The mechanisms underlying gut development, especially peristalsis, are widely studied topics. However, the causes of gut peristalsis-related diseases, especially Opioid-Induced Bowel Dysfunction (OIBD) disorder, have not been well defined. Therefore, our study used zebrafish, a popular model for studying both gut development and peristalsis, and DCFH-DA, a dye that clearly labels the live fish gut lumen, to characterize the formation process of gut lumen as well as the gut movement style *in vivo*. By applying Loperamide Hydrochloride (LH), the  $\mu$ -opioid receptor-specific agonist, we established an OIBD-like zebrafish model. Our study found that acetylcholine (ACh) was a key transmitter that derepressed the phenotype induced by LH. Overall, the study showed that the antagonistic role of ACh in the LH-mediated opioid pathway was evolutionarily conserved; moreover, the OIBD-like zebrafish model will be helpful in the future dissection of the molecular pathways involved in gut lumen development and pathology.

Gut mobility is integral for food digestion and nutrient absorption during one's lifetime. Defects in this process are responsible for severe congenital disorders, such as Hirschsprung's disease<sup>1</sup>; therefore, the molecular mechanisms involved have been extensively studied for several years. Although some "myogenic patterns" of intestinal motility in the intestinal muscles could be revealed in the primary stages of gut movement formation<sup>2</sup>, the enteric nervous system (ENS) is known to be the key neuron system modulating gut mobility. The ENS, which functions independently of the central nervous system (CNS), originates from the agal (post-otic) neural crest<sup>1</sup>. Initially, the vagal neural crest cells enter the foregut and subsequently colonize the whole length of the intestine in a rostro-caudal direction<sup>1,3</sup>. Following the establishment of the ENS, the regular intestinal mobility is established, allowing food ingestion and gut microbiota formation. Although the ENS is primarily responsible for the motility patterns, the interstitial cells of Cajal (ICC) are now recognized as the pacemaker of the regular propagating contractions<sup>2,4,5</sup>. BMP, FGF, Hedgehog (HH), Retinoic Acid (RA), WNT and Notch signals pathways are essential for this process<sup>6–10</sup>.

Similar to the paradigm of the CNS, the integrated ENS circuitry controlling intestinal mobility depends on the orchestration of several groups of transmitters and neuropeptides, such as acetylcholine (ACh), substance P, nitric oxide (NO), adenosine triphosphate, vasoactive intestinal polypeptide, 5-hydroxytryptamine and opioid peptides<sup>11</sup>. The role of opioids has attracted increasing attention because several types of opioid receptors agonists, such as morphine and loperamide, may cause Opioid-Induced Bowel Dysfunction (OIBD) as a side effect. Numerous studies have reported that these agonists interact with opioid pathways in ENS to disrupt gastrointestinal (GI) motility and secretion<sup>12–14</sup> when they are administered to alleviate pain in the CNS. Three types of opioid receptors— $\mu$ ,  $\delta$  and  $\kappa$ —have been identified in human GI tract. The  $\mu$ -opioid receptor plays a major role in the inhibition of gut transit, and its agonist, loperamide, is widely used to treat acute and chronic diarrhea<sup>11,15,16</sup>. Through extensive study, scientists have discovered that the cellular effects of  $\mu$ -opioid receptor depend on multiple transduction pathways, such as the activation of potassium channels, membrane hyperpolarization, inhibition of calcium channels and reduced production of cyclic adenosine monophosphate<sup>16</sup>, eventually result in a reduction of acetylcholine release, with an overall inhibitory effect on neurons<sup>17</sup>. Although  $\mu$ -opioid receptors are the principal mediators of the analgesic action of endogenous and exogenous opioids, they account for the main side effects of OIBD, including symptoms such as sedation, bowel dysfunction, constipation and respiratory depression<sup>18</sup>. Therefore, searching for appropriate chemicals to antagonize the side effects induced by  $\mu$ -opioid receptors in the gut is an important goal.



Acetylcholine is a well-known excitatory neurotransmitter that mainly acts on nicotinic acetylcholine receptors (nAChRs) in both the peripheral nervous system (PNS) and the CNS<sup>19,20</sup>. It is synthesized by choline acetyltransferase and broken down by acetylcholinesterase (AChE)<sup>21</sup>. It exerts multiple functions in the body, with inhibitory effects in cardiac tissue and excitatory roles at neuromuscular junctions in skeletal muscle. In the ENS, it has been known for some time to be the principal excitatory neurotransmitter<sup>19</sup>. Administration of exogenous acetylcholine promotes gut mobility via the stimulation of fast excitatory synaptic transmission by acting at the nicotinic cholinergic receptors<sup>22</sup>.

Recently, zebrafish (*Danio rerio*) has become an increasingly popular model to study vertebrate development, especially for the dissection of early intestinal development and establishment of gut movement<sup>23–28</sup>, based on its rapid extra-uterine development, optical transparency and large numbers of progeny, which are suitable characteristics for large genetic and chemical screening, etc. Spontaneous, propagating gut contractions first appear in zebrafish at 3.5 days post-fertilization (dpf), just before the onset of feeding (5–6 dpf). Similar to higher vertebrates, the zebrafish ENS is derived from the vagal neural crest and instructs gut motility after building up<sup>25</sup>. Additionally, the ICC is still responsible for the regular propagating waves<sup>25,29,30</sup>. However, subtle differences do exist between zebrafish and higher vertebrates. For example, the structure of the gut is relatively simple and the intrinsic innervation between the ENS is less complex in zebrafish<sup>25</sup>. In a coordinated fashion, zebrafish enteric neural crest-derived cells (ENCDCs) colonize the intestinal tract via two parallel chains style, not via the multiple chains used by higher counterparts during the ENS formation<sup>25</sup>. Several types of transmitters have also been discovered in zebrafish recently, including acetylcholine, vasoactive intestinal polypeptide (VIP), calcitonin gene-related polypeptide (CGRP), nitric oxide (NO), neurokinin-A (NKA), serotonin, etc.<sup>23,25,31</sup>. However, little information about  $\mu$ -opioid receptors, especially their roles in gut movement, has been reported. Similarly, the  $\mu$ -opioid receptor-mediated OIBD, which has been thoroughly studied in mouse and pig, remains a novel topic in zebrafish. This situation is likely due to the limitations of easily manipulated methods that allow for detection of gut peristalsis, although several papers have reported progress regarding insight into gut peristalsis type and establishing a time-window via either directed observation or feeding with fluorescent-labeled particles<sup>23,28,29</sup>.

In this study, we developed a convenient method to visualize the intestine in early development and, more importantly, intestinal peristalsis at high resolution by taking advantage of DCFH-DA, a fluorescent probe specifically measuring cell-derived  $H_2O_2$ <sup>32</sup> at low concentrations. The data indicate that this dye has no detectable toxic effects on fish development at the concentration we used, which was approximately 20 times lower than what was used previously<sup>33</sup>. Our results showed that the intestinal bulb primordium could be initially detected as early as 1.5 dpf by weak staining; this quickly became stronger and more obvious at 2 dpf when the gut lumen is initially formed. Further study indicated that DCFH-DA could function as a useful indicator of gut peristalsis as well as the formation of a functional anus. Using this method, we first reported the roles of  $\mu$ -opioid receptors in larval gut peristalsis by treating fish with loperamide, a specific  $\mu$ -opioid receptor agonist that could induce OIBD. Interestingly, further study demonstrated *in vivo* that the inhibited role of loperamide in gut movement was mediated by the suppression of acetylcholine production but not the ablation of ENS neurons. Additionally, the application of exogenous acetylcholine chloride (ACh-Cl) could rescue the loperamide-induced phenotype. Therefore, our study first addressed the function of  $\mu$ -opioid receptor in early zebrafish intestinal mobility and established a zebrafish OIBD model. Additionally, we uncovered the conserved roles of acetylcholine as the antagonist in this pathway *in vivo*.

## Results

**Intestinal lumen formation is easily detected via DCFH-DA staining.** When DCFH-DA, a fluorescent probe specific to  $H_2O_2$ <sup>32</sup>, was administered to larval fish at 3 dpf for 12 hours, to our surprise the dye clearly labeled the whole intestinal tract (Figure 1c1 and 1c2. Red arrows and arrowheads), although it also weakly stained the whole body. The tract was labeled even when the concentration was reduced to 1 mg/L, a level that showed no detectable toxic effects on embryonic development (Figure 1). The simple staining of the intestinal tract with this dye motivated us to investigate the staining patterns at different developmental stages. DCFH-DA labeled the fertilized egg from even the one cell stage with high green color density in the cell (see supplemental Figure S1a), which continued until the germ ring stage (see supplemental Figure S1 b–e). However, this density seemed to localize over the whole body, especially the yolk mucosal epithelium layer, from 12 hpf (see supplemental Figure S1 f–g<sub>2</sub>) until 36 hpf, when the intestinal primordium appeared (see supplemental Figure S1 h, red arrows). Interestingly, this dye clearly labeled the cells circulating pronephric ducts opening at 24 hpf (see supplemental Figure S1 g<sub>1</sub> and g<sub>2</sub>), most likely indicating the presence of apoptotic cells when the opening of pronephric ducts produced large amounts of  $H_2O_2$ . However, from 1.5 dpf onward, the signals began to concentrate in the intestinal bulb (Figure 1a<sub>1</sub> and 1a<sub>2</sub>; see supplemental Figure S1 h, red arrows and arrowheads). From 2 dpf onward, the signals became stronger and several discontinuous small cavities along the intestinal tract appeared, vividly reflecting the intestinal lumen formation process<sup>27</sup> (Figure 1 a<sub>1</sub>–c<sub>1</sub>). The lumens initially appeared in the rostral region near the future intestinal bulb at 2 dpf (Figure 1a<sub>1</sub> and 1a<sub>2</sub>, red arrowheads). Subsequently, the lumens extended caudally as the cavities merged (Figure 1 b<sub>1</sub>) and eventually coalesced to produce a continuous gut hollow tube from 3 dpf onward (Figure 1 c<sub>1</sub>, red arrows). The unopened anus was first observed around this time. From 5 dpf onward, the elaboration of folds, especially in the intestine bulb, was easily visualized in the gut tube (Figure 1 f<sub>1</sub>–f<sub>4</sub>, white arrowheads), suggesting extensive remodeling of the intestinal epithelium. The intestinal configuration was highly analogous to the crypts of Lieberkühn in mammals<sup>26,27</sup>. Interestingly, the opening of the mouth as well as the anus was clearly detectable as the dye was occasionally emitted from the mouth or anus at 4 dpf (Figure 1 g–h, white arrowheads; see supplementary video S1). Additionally, autonomous gut movement was observed from 4 dpf, and the regular spontaneous gut motility could be identified from 5–6 days onwards due to the high resolution of the dye. Interestingly, in addition to staining the gut lumen, the probe also labeled the pronephric ducts (Figure 1 e<sub>1</sub>–e<sub>2</sub>, blue arrows), especially gallbladder clearly from 5 dpf (Figure 1 e<sub>3</sub>–e<sub>4</sub>, white arrows). This feature could serve as a useful platform to study the development of these structures as well.

**DCFH-DA partially marked Duox-dependent ROS in the gut.** The extensive staining of the intestinal lumen by DCFH-DA made us investigate whether this probe reflected the reactive oxygen species (ROS), including  $H_2O_2$ , generated during intestinal development. ROS are highly secreted by the intestine epithelial cells to assist in defense against microbes and maintain the homeostasis of the gut environment; this phenomenon has recently attracted substantial interest<sup>34–36</sup>. Thus, we turned to alamarBlue, another ROS/redox probe<sup>37</sup>. The data indicated that, similar to the action of DCFH-DA, alamarBlue also revealed the process of intestinal lumen formation (Figure 2 a, white arrowheads). However, alamarBlue did not mark the gallbladder or pronephric ducts, although it did label the circulating blood cells (Figure 2 a, white arrows). Luminal staining by both probes suggested that the ROS/redox produced were their labelling targets. To confirm this hypothesis, we blocked *duox*, which is essential for the formation of ROS reagents in the gut<sup>33,34</sup>, via

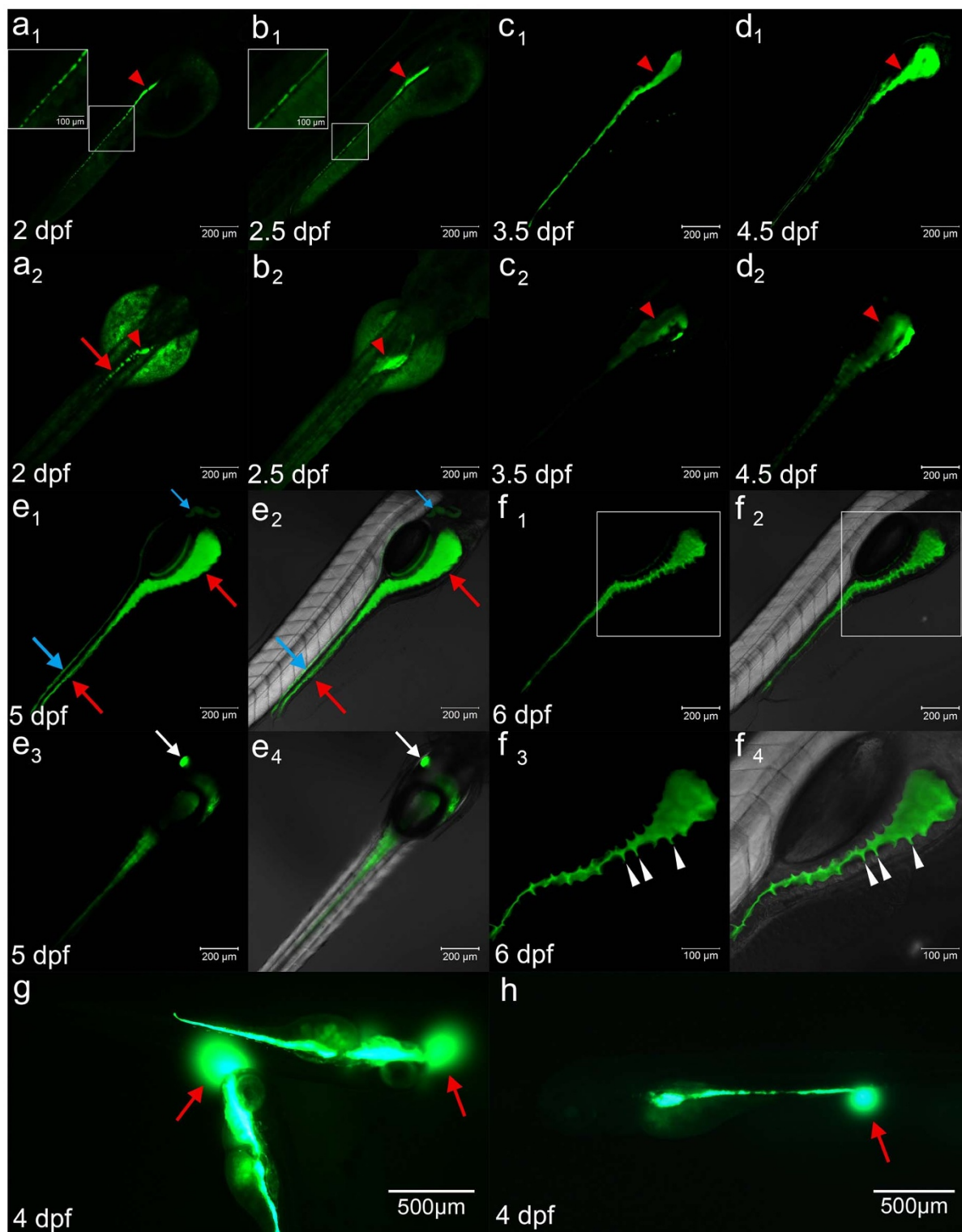


**Figure 1 | DCFH-DA indicates gut lumen development.** (a<sub>1</sub>–d<sub>1</sub>) DCFH-DA reveals the gut lumen formation process at 2–4.5 dpf in the lateral view. (a<sub>2</sub>–d<sub>2</sub>) The dorsal view of the pattern of a<sub>1</sub>–d<sub>1</sub> at 2–4.5 dpf. The red arrows in a<sub>1</sub>–d<sub>2</sub> represent the intestinal lumen formation processes, which initially show a dashed line pattern (boxed region in a<sub>1</sub>–b<sub>1</sub>, red arrows in a<sub>2</sub>) at 2 dpf and merge thereafter. The red arrowheads in a<sub>1</sub> to d<sub>2</sub> indicate the formation of the intestine bulb from 2 dpf, which increases in size at 2.5 dpf (b<sub>1</sub> and b<sub>2</sub>), 3.5 dpf (c<sub>1</sub> and c<sub>2</sub>) and 4.5 dpf (d<sub>1</sub> and d<sub>2</sub>). (e<sub>1</sub>–f<sub>4</sub>) The staining patterns of DCFH-DA at later stages, 5 dpf (e<sub>1</sub>–e<sub>4</sub>) and 6 dpf (f<sub>1</sub>–f<sub>4</sub>). e<sub>1</sub>–e<sub>2</sub> are lateral with regard to the gut after staining, and e<sub>2</sub> is the image of e<sub>1</sub> merged with DIC. The blue arrows in e<sub>1</sub> and e<sub>2</sub> indicate that the dye marks the pronephric ducts in addition to the gut lumen, as indicated by red arrows. e<sub>3</sub>–e<sub>4</sub> shows the dorsal view of the pattern, which indicates that the dye clearly labels the gallbladder (white arrows). e<sub>4</sub> is the image of e<sub>3</sub> merged with DIC. f<sub>1</sub>–f<sub>4</sub> are the lateral views of the gut at 6 dpf, and f<sub>2</sub> and f<sub>4</sub> are the images of f<sub>1</sub> and f<sub>3</sub> merged with DIC. f<sub>3</sub> and f<sub>4</sub> are high magnifications of the boxed images in f<sub>1</sub> and f<sub>2</sub>. The white arrowheads in f<sub>3</sub> and f<sub>4</sub> indicate the folding of the gut epithelium during the formation of crypt-like architecture. (g–h) The dye emitting from the mouth (g) and anus (h). The red arrows represent the circular signals of the emitting dye under the GFP channel.



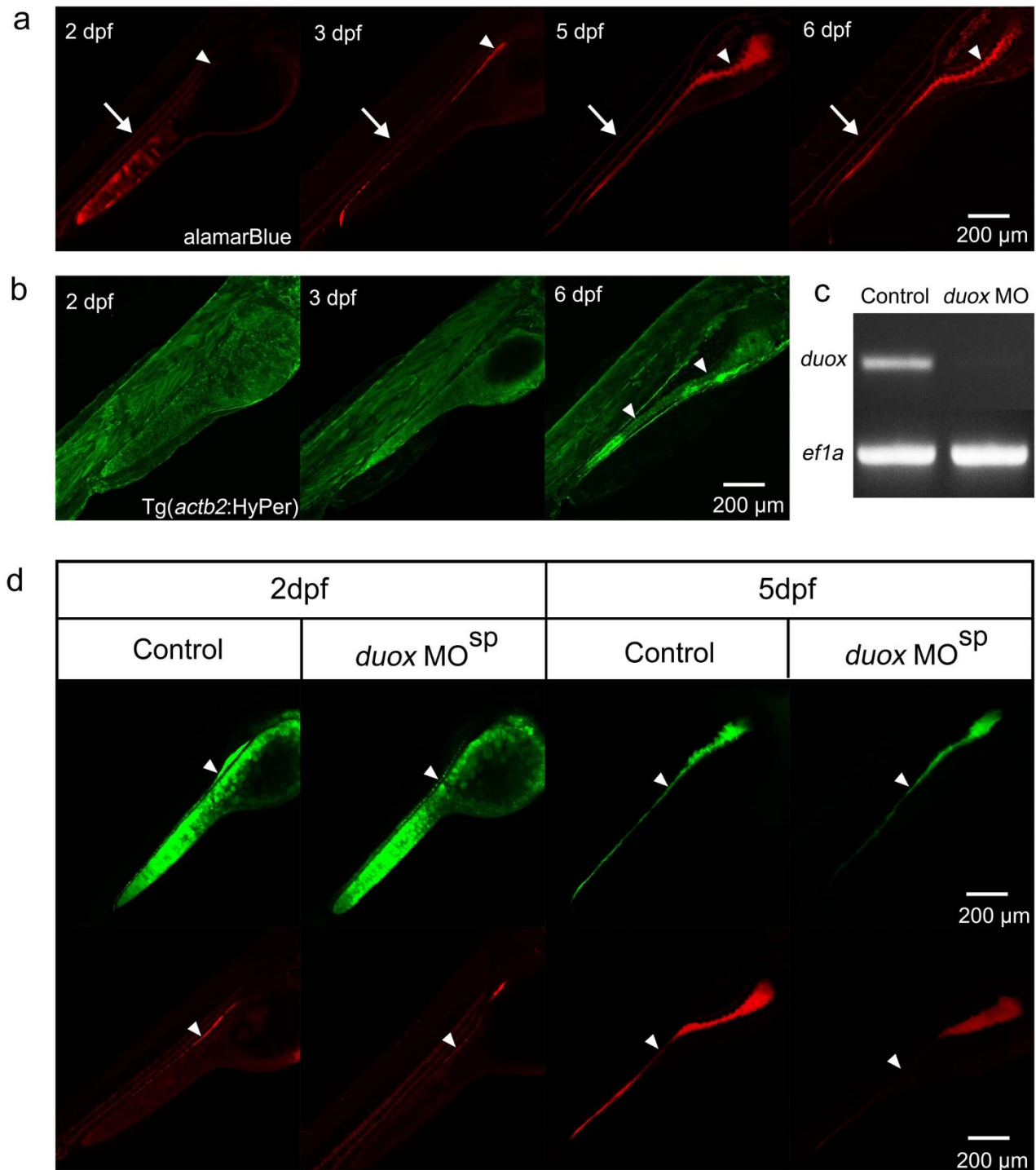


**Figure 2** | DCFH-DA partially marks Duox-dependent ROS in the gut. (a) The staining patterns of alamarBlue reveal the gut lumen (white arrowheads) and circulating blood cells (white arrows) at 2–6 dpf in the lateral view. (b) Green signals are universally detected in Tg(*actb2:HyPer*)*pku326* before 3 dpf, and the signals enhance in the intestinal epithelial cells at 6 dpf (white arrows). (c) RT-PCR reveal the efficient block of *duox* transcript splicing via MO mediated genetic knockdown. (d) The signals of the ROS/redox probes reduce, but not exclusively disappear, in the intestinal tract after *duox* is genetic knockdown by MO. White arrowheads indicate the signals in the intestinal tract.

morpholino (MO)-mediated genetic knockdown. Surprisingly, we detected the fluorescence signals still clearly using both probes, although the signals were largely decreased (Figure 2 d, white arrowheads) following the efficient knockdown of Duox (Figure 2 c). This result suggested that the target of both probes in the gut was not exclusively Duox-dependent ROS. Additionally, we could not exclude the possibility that both probes labeled an additional biological material because Tg(*actb2:HyPer*)*pku326*<sup>38</sup>, a reporter

line of H<sub>2</sub>O<sub>2</sub><sup>39</sup>, did not show obvious signals in the intestine before 3 dpf (Figure 2 b), at which time the fluorescence probes were already quite obvious (Figure 1 c1 and 2 d). At a later stage, however, higher signals were observed in the intestinal epithelial cells of Tg(*actb2:HyPer*)*pku326* (Figure 2 b, white arrowheads).

**DCFH-DA staining is an ideal tool for the study of intestinal peristalsis.** Easy visualization of the gut lumen as well as the

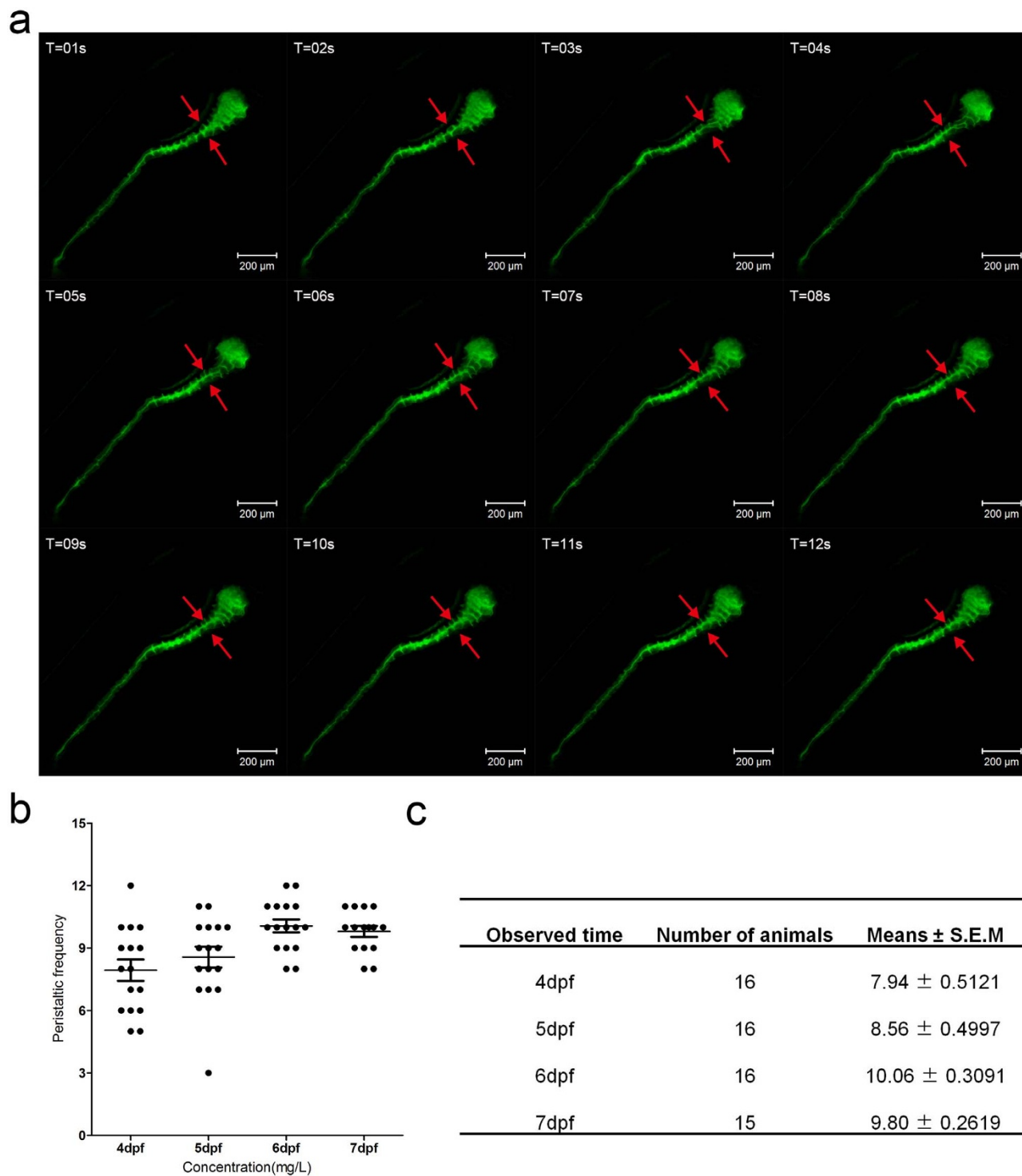


**Figure 3 | Gut peristalsis revealed by live imaging and calculation.** (a) The fragments from the live image (supplement video 2) reveal the gut peristalsis process at 6 dpf larvae fish by DCFH-DA staining, which clearly shows the invaginations of the intestinal bulb epithelium (marked by red arrows). The folding events could serve as an indicator of intestinal movement frequency. (b) Quantification data of the movement frequency at different stages. (c) The table describing the detailed data of b.

feasibility of using DCFH-DA as a tracer indicated that this technique was a useful tool to investigate the characteristics of intestinal peristalsis and the molecules involved. These questions are quite challenging to explore in other model systems due to the difficulty of direct observation. With *in vivo* observation as a goal, we first carefully monitored the movement characteristic of the zebrafish gut under live imaging at 6 dpf (see supplemental video S2). The imaging data clearly revealed that two positions—one near

the intestine bulb and the other close to the anus—generated waves of gut contractions, similar to those observed in previous reports<sup>25,29</sup>. We focused on the contraction waves from the position close to the intestine bulb because this movement frequency could be reliably calculated by counting the invaginations of the bulb epithelium (Figure 3 a, red arrows). Therefore, we used the folding frequency of the bulb epithelium as the indicator for the next study. The results showed that spontaneous gut movement was initially observed from

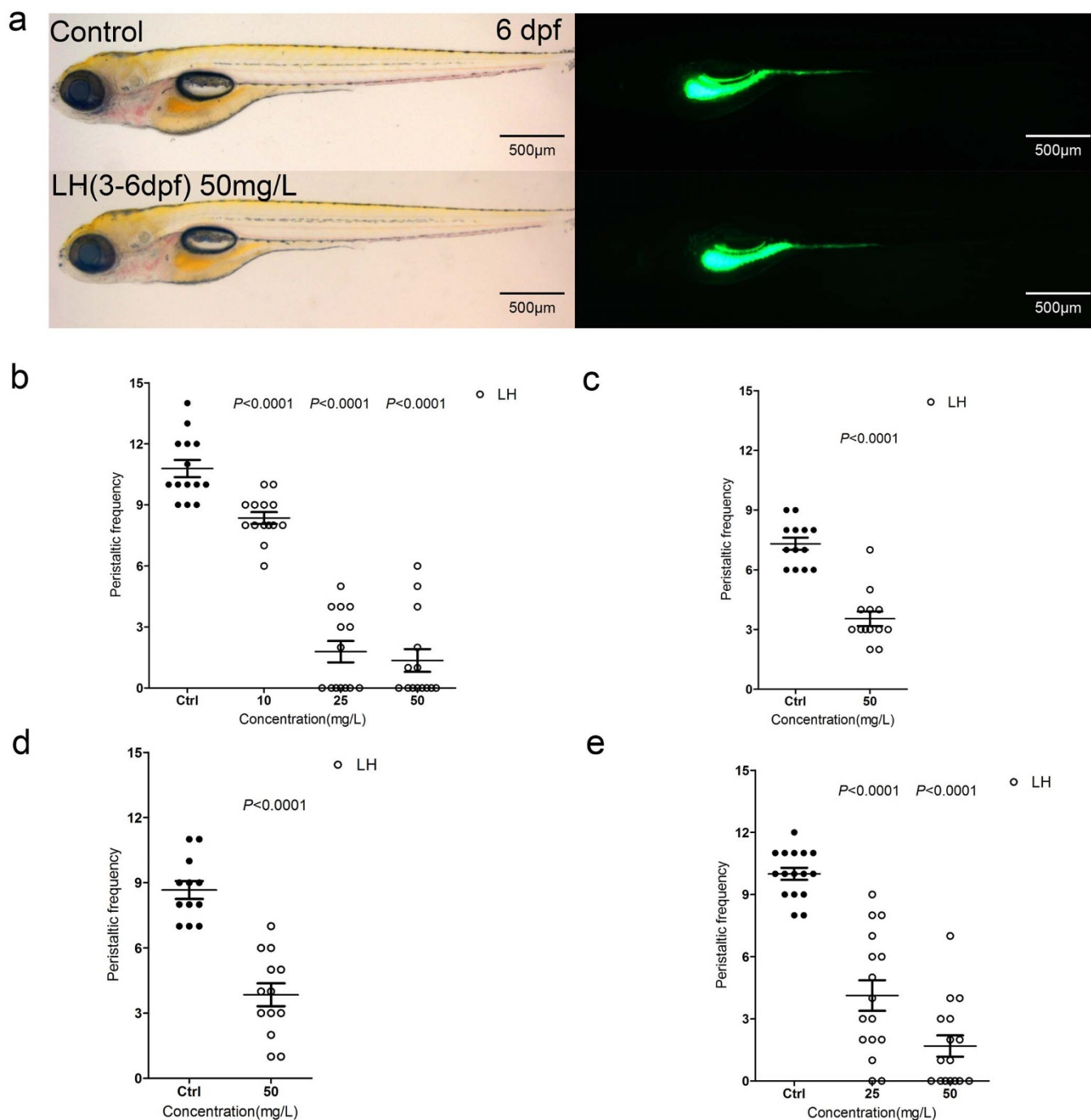


**Figure 4 | LH suppresses the gut peristalsis frequency significantly.** (a) The fish do not show obvious developmental abnormality after treatment of LH for even 3 days compared with control fish. Left panels are in bright field (BF) channel whereas right are in GFP channel. (b) The calculation data uncover the intestinal peristalsis frequency at 6 dpf after application of LH for 3 days. (c–e) The calculation data indicate the effect of LH on gut peristalsis at 4 dpf (c), 5 dpf (d) and 6 dpf (e) after treatment for 12 hours. *P* value is statistical with corresponding control.

4 dpf with high variation between individuals (Figure 3 b and c). However, the rhythm became regular from approximately 5 dpf at approximately  $8.56 \pm 0.50$  times/2 mins. More stable peristalsis frequency was identified from 6 dpf on ( $10.06 \pm 0.31/2$  mins at 6 dpf and  $9.80 \pm 0.26/2$  mins at 7 dpf) (Figure 3 b and c). The gut movement frequency was higher than reported in previous studies<sup>25,29</sup>, most likely because of the different methods used. Additionally, we discovered that dye ejected from the anus accompanied the anterograde contractions (see supplemental video S1). Meanwhile, the dye was occasionally released from the mouth when retrograde contraction began (Figure 1 g, white arrowheads).

Previously, several assays, such as *Tg(gut GFP)s854*<sup>27,40</sup>, a reporter line marking the digestion organ from 26 hpf<sup>27</sup>, and gavage or injection of dextran<sup>41,42</sup>, a fluorescence tracer, were used to study zebrafish larval intestine. Gut mobility was more easily observed in our assay because gutGFP presented weak signals in the gut (see supplemental Figure S2 a, white arrowheads) and because the intensity of fluorescent dextran tracer decreased greatly with time, especially after emission from the anus (see supplemental Figure S2 b). Additionally, the administration of fluorescent tracer by injection or gavage is far more complicated than simple incubation with ROS probes. Overall, this staining assay was shown to be a useful new



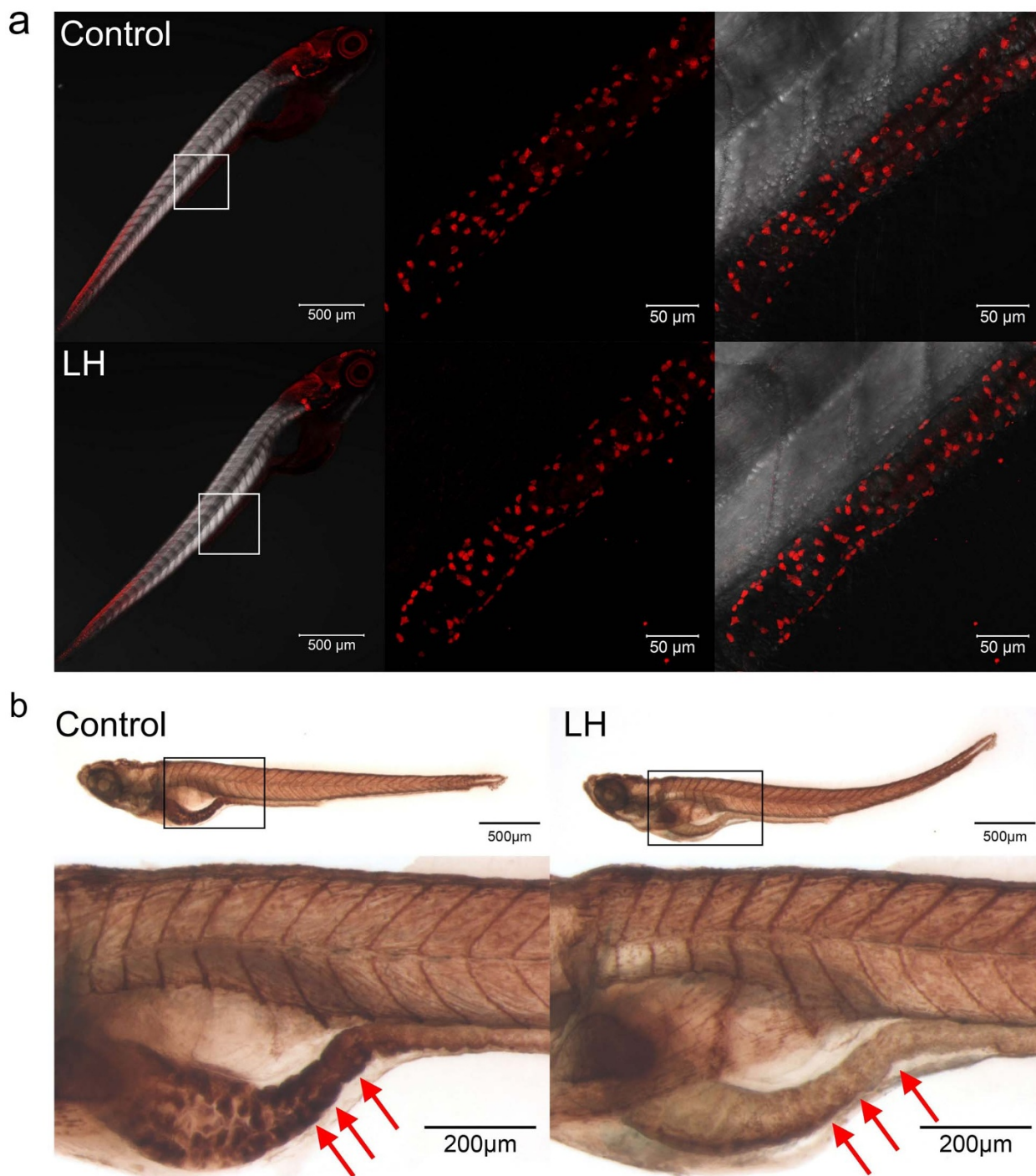


**Figure 5 | LH disrupts AChE activity but not ENS neuron development.** (a) Immunohistochemical staining of HuC/D in both control and LH-treated fish at 6 dpf. The data show no significant difference between the control and chemical application groups. Left panels show the whole body staining pattern of HuC/D, whereas middle and right panels represent high magnifications of the areas that are boxed in left. Right panels are the images of middle merged with DIC. (b) The AChE activity detection assay reveal that AChE activity is significantly reduced after LH treatment (right panels) compared with control (left panels) in the gut but not elsewhere in the body. Upper panels show the whole body staining pattern of Ache, whereas bottom panels represent high magnifications of the boxed images. The red arrows in b indicate the intestinal bulb region where peristalsis is identified.

model for exploring the molecules contributing to the formation and regulation of peristalsis. It also facilitated uncovering the effective but limited side-defect chemicals in the normalization of gut movement rhythm, which could have clinical implications.

**Loperamide hydrochloride (LH) suppressed the gut movement and led to OIBD.** Loperamide is a widely used drug for the treatment of diarrhea that activates the  $\mu$ -opioid receptors in the

myenteric plexus of the large intestine, resulting in the inhibition of gut movement. Another opioid-receptor agonist, morphine, alleviates pain in the CNS. Unfortunately, this type of drug usually induces OIBD. Many recent studies have focused on reducing this unwanted side effect. To this end, we chose to look at loperamide to explore its influence on larval intestine development and peristalsis formation, as well as its ability to induce an OIBD-like syndrome in zebrafish. We first treated the fish embryos with different concen-

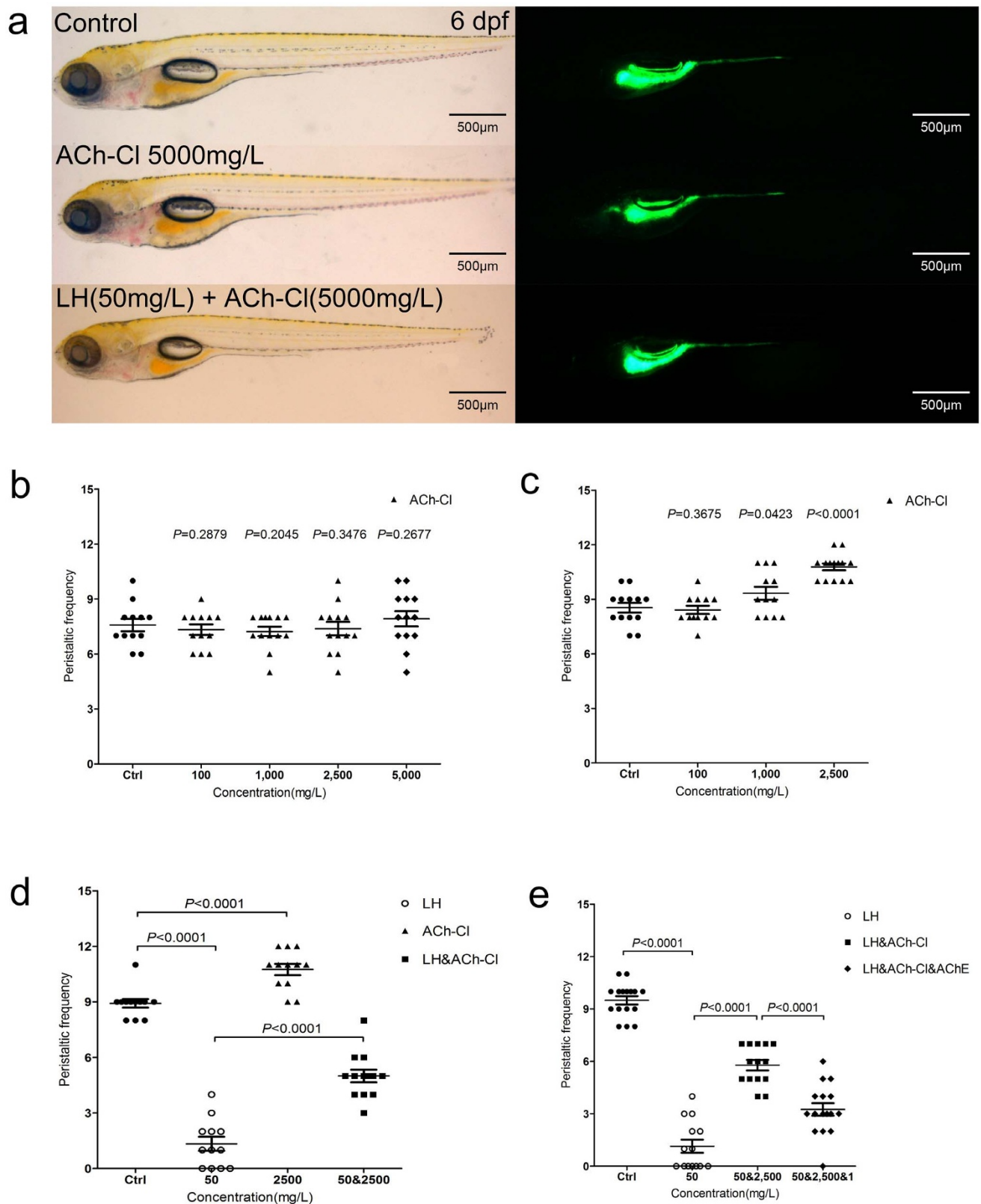


**Figure 6 | Exogenous ACh-Cl partially rescues the LH-induced phenotype.** (a) The larval fish do not show an obvious developmental defect when treated by ACh-Cl and LH+ACh-Cl for 12 hours compared with control. Left panels are in the BF channel, whereas right are in the GFP channel. (b–c) Quantification data indicate that the effect of exogenous ACh-Cl on gut peristalsis at 4 dpf (b) and 6 dpf (c) after transit incubation for 10–30 minutes. 10, 100, 1000, 2500 and 5000 mg/L ACh-Cl had no influence on the gut movement frequency at 4 dpf (b), whereas 2500 mg/L promote the movement ability obviously at 6 dpf (c). (d) Quantification data show that treatment of exogenous ACh-Cl for 10–30 minutes partially rescue the inhibition phenotype of gut peristalsis caused by LH. (e) Quantification data show that acetylcholinesterase (AChE) inhibits the recovered phenotype by exogenous ACh-Cl. *P* value is statistical with corresponding control.





trations of LH at different time points (Figure 4). The data showed that when the chemical was added at 3 dpf for 12 hours, there was no gut mobility with or without LH because gut movement is not initiated before 3.5 dpf (data not shown). However, the administration of this chemical significantly reduced the movement frequency when analyzed at 6 dpf (Figure 4b and Table S1). Moreover, the effect of the chemical was dose-dependent (Figure 4b and Table S1), with 10 mg/L reducing the frequency to  $8.36 \pm 0.29$  and 25 mg/L and 50 mg/L reducing the frequency to  $1.79 \pm 0.53$  and  $1.36 \pm 0.56$  from  $10.79 \pm 0.42$ , respectively, in control groups (Figure 4b and Table S1). However, the larvae did not show any obvious developmental defect (Figure 4a). These data suggest that LH specifically inhibits gut mobility, and the resulting phenotype was quite similar to OIBD<sup>17,43</sup>. To further explore the influence of this chemical, we simplified the protocol to treat the fish embryos for 12 hours with 50 mg/L LH at different time points. The data showed that this level of LH significantly reduced gut mobility during all of the stages tested after gut movement was physiological initiated, and the inhibition effect was more obvious when the larvae were treated during 5.5–6 dpf (Figure 4c–e and Table S1). Interestingly, 50 mg/L of LH significantly influenced the movement frequency in the first 12 hours (Figure 4e and Table S1); however, it was not more effective, despite a longer culture period (Figure 4b, 4e and Table S1) when calculated at 6 dpf. In contrast, the effect of 25 mg/L dosage was correlated with the treatment period: longer treatment periods resulted in more obvious reductions of the frequency (Figure 4b, 4e and Table S1). The calculated data suggested that in addition to the ENS, the  $\mu$ -opioid receptor was set up at the initial stages of the gut development. The repression phenotype of gut mobility resulting from activation of the  $\mu$ -opioid receptor could therefore mimic the OIBD syndrome.

**AChE activity is suppressed under the LH treatment.** The obvious role of LH in the inhibition of intestinal mobility prompted us to investigate the molecules and mechanisms involved. To address this issue, we first examined the ENS neurons in larval fish after chemical application. The ENS neurons were quickly assayed by immunohistochemical testing of HuC/D, a pan-neuronal protein expressed in differentiated neurons<sup>26</sup>. The data revealed that the HuC/D<sup>+</sup> cells in the gut did not show obvious differences compared with control fish after the administration of LH (Figure 5a), suggesting that ENS development was not influenced by this chemical. We next turned to the neurotransmitters. ACh is a well-known neurotransmitter that functions positively in gut movement, and its production was suppressed when LH was used in isolated pig gut<sup>16,17,22</sup>. However, whether the same phenomenon occurs *in vivo* has not been determined. We tested endogenous ACh by assaying AChE activity<sup>44,45</sup>, which hydrolyses ACh and correlates the endogenous ACh level<sup>46–48</sup>. The data showed that AChE activity, especially in the gut bulb, was significantly decreased following LH treatment (Figure 5b, red arrows). These data suggested that AChE activity, but not ENS neurons, was influenced after the  $\mu$ -opioid receptor was agonized.

**ACh is a key neurotransmitter functioning in the  $\mu$ -opioid receptor pathway.** The decreased gut mobility and reduced activity of AChE after LH application led us to investigate whether the administration of exogenous ACh could recover the phenotype. To test this hypothesis, we treated fish larvae with ACh-Cl. Previous studies suggested that treatment with ACh over a short period could promote gut mobility at an early stage (4 dpf), when normal gut movement is first initiated in zebrafish<sup>23</sup>. However, its role at a later stage (6 dpf) had not been reported. When we treated the larvae at 6 dpf for 10–30 minutes with different concentrations, we observed an obvious increase in movement frequency when 2500 mg/L ACh-Cl was used (Figure 6c and Table S1). However, no significant positive efficiency was detected when the larva was treated at 4 dpf (Figure 6b and Table S1) even the dosage up to

5000 mg/L. Interestingly, when the culture time was increased—approximately 12 hours—we did not observe obvious motility differences compared with the control group, even at concentrations up to 5000 mg/L (see supplemental Figure S4c and Table S1). Additionally, this dosage showed no obvious toxicity affecting fish development or the ENS neurons (Figure 6a; see supplemental Figure S3a), although the larvae died within an hour at a dosage of 10000 mg/L (Table S1). The AChE activity decreased largely with longer incubation of ACh-Cl although no obvious difference was detected after transit treatment (see supplemental Figure S3b), this result is most likely because exogenous ACh-Cl exerted a negative feedback effect that suppressed AChE activity<sup>46–48</sup>. Subsequently, we treated the fish with LH and ACh-Cl together at different dosage combinations. The data showed that 50 mg/L of LH reduced the movement frequency to approximately 1/7 ( $1.33 \pm 0.38$ ) of that in control larvae ( $8.92 \pm 0.23$ ) after 12 hours of incubation (Figure 6d and Table S1). Furthermore, this inhibitory phenotype could recover to 1/2 ( $5.00 \pm 0.34$ ) of the control when 2500 mg/L ACh-Cl was added for several minutes (Figure 6f and Table S1). However, longer treatment times with ACh-Cl exhibited a similar recovery phenotype (see supplemental Figure S4d and Table S1), and the recovery ability was dose dependent (see supplemental Figure S4d and Table S1). These data suggested that the ACh-Cl receptors were most likely constant and easily saturated at certain stages. However, the rescue phenotype of ACh-Cl indicated that ACh was indeed a major neurotransmitter functioning against the LH-mediated  $\mu$ -opioid receptor pathway. To confirm this hypothesis, acetylcholinesterase (AChE), the enzyme used to hydrolyze ACh functioning as its inhibitor, was applied. The data indicated that this inhibitor significantly reduced the recovery effect of ACh-Cl on gut mobility (Figure 6d and Table S1). Overall, we believe that the antagonist role of ACh- versus LH-mediated opioid pathway functions in the balanced control of intestinal mobility.

## Discussion

The optical transparency, external development and easy manipulation of zebrafish make this organism a popular model system to study the development of a variety of organs. Research on intestinal development, especially the factors affecting intestinal mobility, has been undertaken by several groups recently<sup>23,24,26–31</sup>. Using WISH, H&E staining, fluorescent-protein marked transgenic lines and fluorescence tracers, previous works have identified the steps involved in intestinal lumen formation, intestinal peristalsis styles, and the ENS formation process as well as several key molecules involved<sup>25–27,29,49–51</sup>, through the merits of both genetic screening and chemical treatment. However, this study is the first to directly describe the lumen formation steps continuously *in vivo* in such clear and high resolution. The gut movement formation and styles at different stages are also described, which could establish an ideal platform for the study of the molecules involved and provide more information about the underlying causes of related diseases, such as Hirschsprung's and OIBD<sup>1,14,17</sup>. The reason that ROS/redox fluorescent probes could so obviously enhance the intestinal lumen remains under investigation, although our present data indicated that the target of the probe was partially the ROS generated via Duox, which could assist in the defense against pathogens and maintain gut homeostasis<sup>35</sup>. However, genetic knockdown of *duox* could not totally erase the signals from ROS probes. Therefore, we could not exclude the possibility that other pathways in the gut control ROS generation. Additionally, it is possible that this dye could non-specifically stain surface of the lumen structure because very weak signals were detected in the gut of *Tg(beta-actin:Hyper)pku326* at 3 dpf (Figure 2B), when the lumen is already extensively stained by ROS probes. Interestingly, work by Annie N.Y. Ng *et al.*<sup>27</sup> indicated that the pan-cytokeratin antibodies, which could reflect the apical surface biogenesis of the larvae gut, showed a pattern similar to those of



the dyes described in our reports. Therefore, we suspect that this dye could label other components secreted by the intestinal epithelium during the formation of the lumen. The characteristics of this dye make it a very helpful tool for the study of the development of the gut lumen, gallbladder, and pronephric ducts, which are located deep inside the body and are difficult to visualize. Additionally, the easy and efficient labeling of the dye makes it an ideal platform for large-scale genetic or chemical screening.

Through careful dissection via our system, we found that the intestinal lumen could be detected as early as 1.5 dpf, first using the technique of disperse points, followed by the ligation of the lumen integrated at 2 dpf, similar to previous reports<sup>27</sup>. This process can be vividly imaged in our system but not via a section of sacrificed larvae. Accompanying gut lumen development, the neuronal system begins to colonize the gut muscle and eventually sets up the ENS. Actually, the initial spontaneous intestine contractions, which are focal, can be first observed at approximately 3.5 dpf in zebrafish larvae, according to a previous study<sup>28</sup>. With the formation of the ICC, the wave begins to propagate along the intestine by 4 dpf, and the rhythmic activity increases over the next several days<sup>24,28,31</sup>. In our study, we also find that the initial spontaneous gut movement starts at approximately 3–4 dpf but is sporadic and irregular, and it is not until 5–6 dpf that the regular periodicity of peristalsis appears. Obviously, this regular contraction derives from the caudal end of the intestinal bulb, with one wave anterior (the retrograde contraction) and the other posterior to the anus (the posterior contraction). Interestingly, the retrograde contractions lead to extensive folding of the bulb epithelium, which most likely mixes food, whereas the posterior contraction appears to be primarily propulsive. Because the deforming of the bulb was easily observed, we selected the intestine bulb invagination frequency at 6 dpf as an indicator of gut mobility. However, the movement frequency reported in our study is much higher than that reported previously<sup>23,24,31</sup>. This discrepancy is most likely due to the different methods used. Additionally, the use of different experimental conditions could lead to this movement difference. Temperature may have an especially large effect; we found that when the temperature decreased slightly, the movement frequency was significantly reduced (data not shown). However, our study reports similar peristalsis initiation time points, movement alteration process and style compared to previous studies<sup>23–25,29,31</sup>. Furthermore, our study clearly identifies the open period of the anus and the emitting style of the dye via anus or mouth, which could help establish an improved system for the study of gastrointestinal physiology, especially the molecules involved in intestinal transit.

It is now known that the ENS system is formed at approximately 3 dpf in the zebrafish intestine<sup>25,29</sup>, which functions thereafter through several types of transmitters, such as Ach, serotonin (5-HT), vasoactive intestinal peptide (VIP) and nitric oxide (NO)<sup>25</sup>. The  $\mu$ -opioid receptor is very important in both the CNS and ENS. It functions as the major target to alleviate pain in the CNS and also suppresses GI mobility in the ENS<sup>11,14,15,25</sup>. However, continued activation of this receptor usually leads to OIBD as a side effect<sup>12–14</sup>. Therefore, discovering a method to extend its function in the CNS while also restricting its side effects is the goal. In zebrafish, the  $\mu$ -opioid receptor functions from 3.5–4 dpf because the administration of its agonist, LH, could extensively inhibit intestinal mobility. This is the first time that the function of the  $\mu$ -opioid receptor has been shown in the zebrafish intestinal tract. Additionally, the suppression of gut movement by continuous administration of LH could clinically mimic OIBD and could represent a useful zebrafish OIBD model for further study.

It has been reported that *in vitro*, the suppressive role of loperamide in GI movement is mediated by reduced secretion of ACh when the opioid receptor is activated<sup>16,17,22</sup>. However, whether this is also the case *in vivo* has not been addressed. Our current study proved that in zebrafish, activation of the  $\mu$ -opioid receptor by LH sup-

presses AChE activity but not ENS neuron development, which might reflect reduced endogenous Ach<sup>46–48</sup>. Similarly, previous studies indicated that exogenous treatment with ACh could accelerate gut movement at the initial stage<sup>23</sup>, which suggests that the cholinergic neuron is formed and functioning just after the gut lumen is formed. In our study, we also observed the stimulatory effect of ACh-Cl when administered for a short time, although this effect was not obvious at early stages (4dpf). However, this phenotype is not seen with a longer culture period, suggesting that negative feedback is used by the organism to maintain homeostasis during a longer treatment, similar to the results of a previous study<sup>46–48</sup>. Coordinately, we detected decreased AChE activity after longer time of chemical application, especially when LH&ACh-Cl were used together (see supplemental Figure S3 e–h), this result suggest that the repressed AChE activity is enhanced by exogenous ACh-Cl induced negative feedback. Additionally, ACh functioned as a key neurotransmitter, especially when the  $\mu$ -opioid receptor was activated. When exogenous ACh-Cl was restored, the movement frequency could partially recover to its normal condition after LH treatment. This recovery effect is disrupted again with the application of its inhibitor. These rescue data demonstrate that the antagonistic role of ACh versus  $\mu$ -opioid receptor pathway also exists evolutionarily in zebrafish. Overall, the role of neurotransmitters in gut movement during the early stage remains an open question to be explored in the future. This model could function as a useful system for further study of the mechanisms underlying gut movement.

## Methods

**Fish lines.** Wild-type AB, *Tg(actb2:HyPer)pk326*<sup>38</sup>, and *Tg(gut GFP)s854*<sup>40</sup> fish strains were used in this study. All the lines were raised and maintained under standard laboratory conditions and protocols. Embryos were maintained in egg water containing 0.2 mM N-phenylthiourea (PTU) to prevent pigment formation<sup>52</sup>.

**Morpholino (MO) injection and valuation.** The *duox*-MO (5'-TAGATTACTA-CTCACAACAGCTTA-3')<sup>34</sup> (1.6 pmol) and standard control morpholino: (5'-CCTCTTACCTCAGTTACAATTATA-3') (1 pmol) were injected into 1-cell embryos. To verify the efficiency of the MO, semiquantitative reverse-transcribed polymerase chain reaction (RT-PCR)<sup>53</sup> was performed using the following primers: *duox*, 5'-ATGGGTTTCATTGAGCTACTT-3'/5'-GAGAACGCTTCTGTCTTGT-3'; and *efla*, 5'-CTTCTCAGGCTGACTGTGC-3'/5'-CCGTAAGCATTACCCTCC-3'.

**Administration of DCFH-DA, alamarBlue, Dextran, Acetylcholinesterase and chemicals.** Embryos at different stages were incubated with 1 mg/L DCFH-DA (Wako, 029-15381) and alamarBlue (Life Technologies, DAL1025) in PTU egg water. The Dextran (Life Technologies, D-1822) was diluted to 25 mg/ml and injected into the intestinal bulb of the larvae fish at 5 dpf. To study the effects of several chemicals, they were first dissolved in DMSO and then diluted in egg water for incubation. The control group was treated with DMSO at the same concentrations used in the chemical groups. The chemicals used in this study were as follows: Loperamide Hydrochloride (sigma, 34014), Acetylcholine chloride (sigma, A6625), and Acetylcholinesterase (sigma, C3389). The embryos were maintained at 28°C for all experiments.

**Detection of AChE enzymatic activity.** AChE activity was detected mainly with the method mentioned in previous literature<sup>44,45</sup>. Overall, the fixed embryos (6–8 h in BT-fix at room temperature) were first treated by Proteinase K (20 mg/L) for 30 minutes, then they were incubated for 4–5 h in 60 mM sodium acetate buffer pH 6.4, 5 mM sodium citrate, 4.7 mM CuSO<sub>4</sub>, 0.5 mM K<sub>3</sub>(Fe(CN)<sub>6</sub>) and 1.7 mM acetylthiocholine iodide and washed extensively with PBS, 0.1% Tween20 before observation.

### Single fluorescence immunohistochemical staining of HuC/D.

Immunohistochemistry was performed essentially as previously described<sup>54</sup>. To examine the HuC/D (Life Technologies, A21271), the embryos were first stained with HuC/D first antibody (20  $\mu$ g/ml, 4°C, overnight) and were subsequently visualized by Alexa Fluor-555 donkey anti-mouse (Life Technologies, A-31570).

**Live Imaging Analysis.** The whole process was similar as previous one<sup>55</sup>. To visualize the intestinal peristalsis, fish embryos were anesthetized and mounted in 1% agarose and subsequently imaged under an LSM700 confocal microscope (Carl Zeiss) at 28°C incubator. Images were taken every 1 second, extracted, and converted to the movie with ZEN2011 software. Movie maker was used to create the movie. However, to record the process of dye given out from anus, the fish embryos were anesthetized and



put under the SteREO Discovery.V20 microscope, the images were taken live and convert to the movie by ZEN2011 software.

**Scoring gut movement frequency at different stages.** The invaginations of the gut epithelium in the caudal part of intestinal bulb were counted for 2 minutes for each larvae fish at 6 dpf under the GFP channel using SteREO Discovery.V20 microscope. Each embryo was scored twice for all the invaginations frequency, and the average count was calculated, the whole calculation assays were repeated 2–3 times.

**Statistical Methods.** The calculated data were recorded and analyzed by GraphPad Prism 5.0. Student's t test (one tailed) was mainly used as the statistical method.

- Burzynski, G., Shepherd, I. T. & Enomoto, H. Genetic model system studies of the development of the enteric nervous system, gut motility and Hirschsprung's disease. *Neurogastroenterol. Motil.* **21**, 113–127 (2009).
- Anderson, R. B., Enomoto, H., Bornstein, J. C. & Young, H. M. The enteric nervous system is not essential for the propulsion of gut contents in fetal mice. *Gut* **53**, 1546–1547 (2004).
- Burns, A. J. & Douarin, N. M. The sacral neural crest contributes neurons and glia to the post-umbilical gut: spatiotemporal analysis of the development of the enteric nervous system. *Development* **125**, 4335–4347 (1998).
- Sanders, K. M., Koh, S. D. & Ward, S. M. Interstitial cells of cajal as pacemakers in the gastrointestinal tract. *Annu. Rev. Physiol.* **68**, 307–343 (2006).
- Sanders, K. M. A case for interstitial cells of Cajal as pacemakers and mediators of neurotransmission in the gastrointestinal tract. *Gastroenterology* **111**, 492–515 (1996).
- Fu, M., Lui, V. C., Sham, M. H., Pachnis, V. & Tam, P. K. Sonic hedgehog regulates the proliferation, differentiation, and migration of enteric neural crest cells in gut. *J. Cell Biol.* **166**, 673–684 (2004).
- Cacalano, G. *et al.* GFRalpha1 is an essential receptor component for GDNF in the developing nervous system and kidney. *Neuron* **21**, 53–62 (1998).
- Sauka-Spengler, T. & Barenbaum, M. Gain- and loss-of-function approaches in the chick embryo. *Methods Cell Biol.* **87**, 237–256 (2008).
- Goldstein, A. M., Brewer, K. C., Doyle, A. M., Nagy, N. & Roberts, D. J. BMP signaling is necessary for neural crest cell migration and ganglion formation in the enteric nervous system. *Mech. Dev.* **122**, 821–833 (2005).
- Okamura, Y. & Saga, Y. Notch signaling is required for the maintenance of enteric neural crest progenitors. *Development* **135**, 3555–3565 (2008).
- Holzer, P. Opioid receptors in the gastrointestinal tract. *Regul. Pept.* **155**, 11–17 (2009).
- Sanger, G. J. & Tuladhar, B. R. The role of endogenous opioids in the control of gastrointestinal motility: predictions from in vitro modelling. *Neurogastroenterol. Motil.* **16 Suppl 2**, 38–45 (2004).
- Kromer, W. Endogenous and exogenous opioids in the control of gastrointestinal motility and secretion. *Pharmacol. Rev.* **40**, 121–162 (1988).
- Holzer, P. Opioids and opioid receptors in the enteric nervous system: from a problem in opioid analgesia to a possible new prokinetic therapy in humans. *Neurosci. Lett.* **361**, 192–195 (2004).
- Baldi, F., Bianco, M. A., Nardone, G., Pilotto, A. & Zamparo, E. Focus on acute diarrhoeal disease. *World J. Gastroenterol.* **15**, 3341–3348 (2009).
- Wood, J. D. & Galligan, J. J. Function of opioids in the enteric nervous system. *Neurogastroenterol. Motil.* **16 Suppl 2**, 17–28 (2004).
- De Schepper, H. U., Cremonini, F., Park, M. I. & Camilleri, M. Opioids and the gut: pharmacology and current clinical experience. *Neurogastroenterol. Motil.* **16**, 383–394 (2004).
- Pasternak, G. W. Pharmacological mechanisms of opioid analgesics. *Clin. Neuropharmacol.* **16**, 1–18 (1993).
- Galligan, J. J. Pharmacology of synaptic transmission in the enteric nervous system. *Curr. Opin. Pharmacol.* **2**, 623–629 (2002).
- Galligan, J. J., LePard, K. J., Schneider, D. A. & Zhou, X. Multiple mechanisms of fast excitatory synaptic transmission in the enteric nervous system. *J. Auton. Nerv. Syst.* **81**, 97–103 (2000).
- Harrington, A. M., Hutson, J. M. & Southwell, B. R. Cholinergic neurotransmission and muscarinic receptors in the enteric nervous system. *Prog. Histochem. Cytochem.* **44**, 173–202 (2010).
- Schneider, D. A. & Galligan, J. J. Presynaptic nicotinic acetylcholine receptors in the myenteric plexus of guinea pig intestine. *Am. J. Physiol. Gastrointest. Liver Physiol.* **279**, G528–G535 (2000).
- Holmberg, A., Schwerte, T., Pelster, B. & Holmgren, S. Ontogeny of the gut motility control system in zebrafish *Danio rerio* embryos and larvae. *J. Exp. Biol.* **207**, 4085–4094 (2004).
- Holmberg, A., Olsson, C. & Hennig, G. W. TTX-sensitive and TTX-insensitive control of spontaneous gut motility in the developing zebrafish (*Danio rerio*) larvae. *J. Exp. Biol.* **210**, 1084–1091 (2007).
- Shepherd, I. & Eisen, J. Development of the zebrafish enteric nervous system. *Methods Cell Biol.* **101**, 143–160 (2011).
- Wallace, K. N., Akhter, S., Smith, E. M., Lorent, K. & Pack, M. Intestinal growth and differentiation in zebrafish. *Mech. Dev.* **122**, 157–173 (2005).
- Ng, A. N. *et al.* Formation of the digestive system in zebrafish: III. Intestinal epithelium morphogenesis. *Dev. Biol.* **286**, 114–135 (2005).
- Kuhlman, J. & Eisen, J. S. Genetic screen for mutations affecting development and function of the enteric nervous system. *Dev. Dyn.* **236**, 118–127 (2007).
- Field, H. A., Kelley, K. A., Martell, L., Goldstein, A. M. & Serluca, F. C. Analysis of gastrointestinal physiology using a novel intestinal transit assay in zebrafish. *Neurogastroenterol. Motil.* **21**, 304–312 (2009).
- Rich, A. *et al.* Kit signaling is required for development of coordinated motility patterns in zebrafish gastrointestinal tract. *Zebrafish.* **10**, 154–160 (2013).
- Holmberg, A., Olsson, C. & Holmgren, S. The effects of endogenous and exogenous nitric oxide on gut motility in zebrafish *Danio rerio* embryos and larvae. *J. Exp. Biol.* **209**, 2472–2479 (2006).
- Maeda, H. *et al.* Fluorescent probes for hydrogen peroxide based on a non-oxidative mechanism. *Angew. Chem. Int. Ed Engl.* **43**, 2389–2391 (2004).
- Niethammer, P., Grabher, C., Look, A. T. & Mitchison, T. J. A tissue-scale gradient of hydrogen peroxide mediates rapid wound detection in zebrafish. *Nature* **459**, 996–999 (2009).
- Flores, M. V. *et al.* Dual oxidase in the intestinal epithelium of zebrafish larvae has anti-bacterial properties. *Biochem. Biophys. Res. Commun.* **400**, 164–168 (2010).
- Ha, E. M., Oh, C. T., Bae, Y. S. & Lee, W. J. A direct role for dual oxidase in *Drosophila* gut immunity. *Science* **310**, 847–850 (2005).
- Rokutan, K. *et al.* Nox enzymes and oxidative stress in the immunopathology of the gastrointestinal tract. *Semin. Immunopathol.* **30**, 315–327 (2008).
- Erikstein, B. S. *et al.* Cellular stress induced by resazurin leads to autophagy and cell death via production of reactive oxygen species and mitochondrial impairment. *J. Cell Biochem.* **111**, 574–584 (2010).
- Yan, B. *et al.* IL-1beta and Reactive Oxygen Species Differentially Regulate Neutrophil Directional Migration and Basal Random Motility in a Zebrafish Injury-Induced Inflammation Model. *J. Immunol.* (2014).
- Belousov, V. V. *et al.* Genetically encoded fluorescent indicator for intracellular hydrogen peroxide. *Nat. Methods* **3**, 281–286 (2006).
- Field, H. A., Ober, E. A., Roeser, T. & Stainier, D. Y. Formation of the digestive system in zebrafish. I. Liver morphogenesis. *Dev. Biol.* **253**, 279–290 (2003).
- Cocchiaro, J. L. & Rawls, J. F. Microgavage of zebrafish larvae. *J. Vis. Exp.* e4434 (2013).
- Goldsmith, J. R., Cocchiaro, J. L., Rawls, J. F. & Jobin, C. Glafenine-induced intestinal injury in zebrafish is ameliorated by mu-opioid signaling via enhancement of Atf6-dependent cellular stress responses. *Dis. Model. Mech.* **6**, 146–159 (2013).
- Brock, C. *et al.* Opioid-induced bowel dysfunction: pathophysiology and management. *Drugs* **72**, 1847–1865 (2012).
- Karnovsky, M. J. & Roots, L. A. “Direct-coloring” thiocholine method for cholinesterases. *J. Histochem. Cytochem.* **12**, 219–221 (1964).
- Behra, M. *et al.* Acetylcholinesterase is required for neuronal and muscular development in the zebrafish embryo. *Nat. Neurosci.* **5**, 111–118 (2002).
- Sarter, M., Parikh, V. & Howe, W. M. Phasic acetylcholine release and the volume transmission hypothesis: time to move on. *Nat. Rev. Neurosci.* **10**, 383–390 (2009).
- Soreq, H. & Seidman, S. Acetylcholinesterase—new roles for an old actor. *Nat. Rev. Neurosci.* **2**, 294–302 (2001).
- Kilbinger, H. & Wessler, I. Inhibition by acetylcholine of the stimulation-evoked release of [<sup>3</sup>H]acetylcholine from the guinea-pig myenteric plexus. *Neuroscience* **5**, 1331–1340 (1980).
- Ball, E. R. *et al.* Ultra-structural identification of interstitial cells of Cajal in the zebrafish *Danio rerio*. *Cell Tissue Res.* **349**, 483–491 (2012).
- Seiler, C., Abrams, J. & Pack, M. Characterization of zebrafish intestinal smooth muscle development using a novel sm22alpha-b promoter. *Dev. Dyn.* **239**, 2806–2812 (2010).
- Pietsch, J. *et al.* *lessen* encodes a zebrafish trap100 required for enteric nervous system development. *Development* **133**, 395–406 (2006).
- Westerfield, M. *The zebrafish book: a guide for the laboratory use of zebrafish (Danio rerio)* (Westerfield, M. [Eugene, OR] 1995).
- Li, L., Jin, H., Xu, J., Shi, Y. & Wen, Z. Irf8 regulates macrophage versus neutrophil fate during zebrafish primitive myelopoiesis. *Blood* **117**, 1359–1369 (2011).
- Wallace, K. N. & Pack, M. Unique and conserved aspects of gut development in zebrafish. *Dev. Biol.* **255**, 12–29 (2003).
- Li, L., Yan, B., Shi, Y. Q., Zhang, W. Q. & Wen, Z. L. Live imaging reveals differing roles of macrophages and neutrophils during zebrafish tail fin regeneration. *J. Biol. Chem.* **287**, 25353–25360 (2012).

## Acknowledgments

We thank Dr. Z. Wen, Dr. J. Xiong, Dr. B. Yan and Miss T. Wang for fish lines, morpholinos, plasmids and discussions. This work was supported by the Natural Science Foundation of China (31271568 and 31301198), the special fund of Chongqing key laboratory (CSTC); the Par-Eu Scholars Program (SWU112015) and The Fundamental Research Funds for the Central Universities.

## Author contributions

Y.S. and L.L. designed the experiments. Y.S., Y.Z. and F.Z. performed most experiments, L.L. wrote the manuscript, L.L., H.H. and H.R. discussed the results and commented on the manuscript.





## Additional information

Supplementary information accompanies this paper at <http://www.nature.com/scientificreports>

**Competing financial interests:** The authors declare no competing financial interests.

**How to cite this article:** Shi, Y. *et al.* Acetylcholine serves as a derepressor in Loperamide-induced Opioid-Induced Bowel Dysfunction (OIBD) in zebrafish. *Sci. Rep.* 4, 5602; DOI:10.1038/srep05602 (2014).



This work is licensed under a Creative Commons Attribution-NonCommercial-NoDerivs 4.0 International License. The images or other third party material in this article are included in the article's Creative Commons license, unless indicated otherwise in the credit line; if the material is not included under the Creative Commons license, users will need to obtain permission from the license holder in order to reproduce the material. To view a copy of this license, visit <http://creativecommons.org/licenses/by-nc-nd/4.0/>